

Implementation of the new cloud-radiation scheme in COSMO

PAVEL KHAIN¹, HAREL MUSKATEL¹ and ULRICH BLAHAK²

¹*Israel Meteorological Service*

²*Deutscher Wetterdienst*

1 Introduction

Incoming solar radiation is a primary driving source of atmospheric weather and climate processes. For realistic weather simulation, an NWP model has to include an appropriate parametrization of the radiative transfer through the atmosphere. The divergence of solar and thermal radiative fluxes in the atmosphere, which interact strongly with gases, aerosols and the simulated cloud field and its inherent properties, contributes considerably to the diabatic forcing in the prognostic model equations. At the earth's surface radiative fluxes constitute the major forcing for the thermodynamic state of the soil and the interaction with the atmosphere via turbulent fluxes of heat and moisture. In COSMO, the radiative transfer scheme is based on the solution of the δ -two-stream version of the radiative transfer equation incorporating the effects of scattering, absorption, and emission by cloud droplets and ice crystals, gases (water vapor, ozone, carbon dioxide, air molecules) and aerosols in each one of the eight spectral intervals [15, 3]. Optical properties are computed from relevant prognostic and/or diagnostic model variables like specific humidity, cloud water- and ice content and cloud fraction. Some layer properties, like ozone, carbon dioxide and aerosols are specified as climatological values. In particular, the spatially variable aerosol distribution is derived from a climatology provided by Tanre [17] (namelist parameter `itype_aerosol=1`). The actual layer mean values of optically relevant substances are converted to radiative properties like optical depth τ , single scattering albedo ω and asymmetry parameter g and forward-scattered fraction through the use of empirical relations described in [15]. As part of the COSMO priority project "Testing and Tuning of the Revised Cloud Radiation Coupling" $T^2(RC)^2$, the calculation of the optical properties at the model layers was significantly revised, and an additional version of a radiative solver was implemented. From a technical point of view, the new parametrizations can be activated via compilation with the "DCLOUDRAD" preprocessor flag. The changes can be divided into three topics: radiative solver, clear sky optical properties, and cloudy part optical properties.

2 Implementation of the new scheme

Radiative solver

Radiation transfer schemes are one of the most computational expensive components in numerical weather prediction (NWP) models. In COSMO model, with only eight spectral intervals, a full radiation calculation costs as much as eight times the cost of the entire COSMO model run. Most of NWP models compromise on the spatial and/or temporal resolution of the radiation scheme. In the operational setup of COSMO-2.8 km, with a full spatial resolution and with a temporal resolution of 15 minutes, the computational cost of radiation is only 3% of the entire model. This compromise can lead to local biases in net downward radiation and surface temperatures. In an attempt to both reduce errors and to decrease the run-time we implemented a different approach which is to decrease the spectral resolution by a wise sampling technique, a method known as Monte Carlo Spectral Integration (MCSI) [13] was implemented (namelist parameter `itype_mcsi`). Many radiative transfer schemes including COSMO scheme [15], use the k-distribution method for the gases-radiation interaction calculations [4]. In this method the spectrum is transferred from wavelength space to cumulative probability space. This space is divided to intervals which are called g-points. In COSMO for each gas and for each spectral interval there are between two to eight g-points. In the operational mode of COSMO the Fast Exponential Sum Fitting Technique (FESFT) is used to fully calculate all of the mentioned g-points. In MCSI only one g-point is calculated in each time step according to its probability. In COSMO we used a softer version of MCSI where a g-point is selected in each of the spectral intervals which increases the computational cost but does neglect either of the spectral intervals in every time step. Of course that if the user chooses to use MCSI the radiation scheme should be called more frequently. We found out the using the MCSI with full temporal resolution (calling the radiation scheme every time step) in COSMO-2.8km setup can increase runtime by 33% with only slight reduction of global radiation and 2-meter temperature biases compared to FESFT. But using MCSI with a 100 seconds temporal resolution (every 5 time steps) can give the same benefits but with only 4% increase in runtime.

Clear sky optical properties

Two new options of an aerosol climatology were introduced (namelist parameter `itype_aerosol`). The first, Tegen [18] (`itype_aerosol=2`), is a 2-dimensional monthly map of optical thicknesses for 5 aerosol classes. In COSMO it is interpolated in time, and 3-dimensional optical properties are calculated assuming a predefined exponentially decaying vertical profile. The second, Kinne [10] (`itype_aerosol=3`), is a 2-dimensional climatology which is considered to better describe real aerosol loading [12].

In addition, two new options to use time- and space-interpolated (via the `int2lm` software) 3-dimensional aerosol fields of external prognostic forecast models have been implemented. The first (`itype_aerosol=4`) can process CAMS-ECMWF [1, 11] 3-dimensional aerosol mixing ratio fields, which include sea salt, mineral dust, black carbon, organic matter and sulphate and which are sub-divided to eleven tracers, because sea salt and dust have three size bins while black carbon and organic matter have both hydrophobic and hydrophilic types. The second new option (`itype_aerosol=5`) can process ICON-ART [14] 3-dimensional aerosol mixing ratio fields; currently the operational ICON-ART only includes mineral dust, but it might be expanded to other species in the future.

Cloudy part optical properties

First, in addition to cloud water and ice, the optical effect of prognostic snow, graupel and rain water contents was (optionally) included (namelist parameter `lrad_incl_qrqsqg`). The optical properties of solid particles in clouds (specific extinction coefficient β , single scattering albedo ω , asymmetry factor g and delta-transmission function δ) have been formulated as function of effective radius R_e and aspect ratio A_r (assuming hexagonal needles as described in [5]) for the 8 COSMO spectral bands, using the spectroscopic scattering function data for single needles used previously in [5], [6] and [7]. Based on these data, for each realization of a Monte-Carlo-Ensemble over 7000 different Gamma-type ice particle size distributions the parameters R_e following [5], A_r following [7], β , ω , g and δ have been computed. New and rather accurate fits of type rational functions were developed for β and ω as function of R_e , and g and δ as function of A_r ([7]). In contrast to previous literature, our new fits span a very large parameter range for R_e from 2.5 to 300 microns and behave asymptotically “reasonably well” for larger sizes. This range is sufficient for the fits to be applied to the snow- and graupel hydrometeors in any model. Optical thickness τ is obtained by multiplying the respective β for each hydrometeor type by the respective specific mass content and summation. Usage of the new fits can be activated by namelist parameter `lradpar_cloud=4`, and small modifications can be chosen by the namelist switches `lrad_ice_smooth_surfaces` and `lrad_ice_fd_is_gsq`.

The optical properties of water particles in clouds have been formulated as function of particles' water content and effective radius for the 8 COSMO spectral bands, using [8] up to 60 micron with an own asymptotically correct extrapolation towards larger sizes up to mm diameters (namelist parameter `lradpar_cloud=4`).

For the large particles (snow, graupel and rain) a geometrical-optics large-size approximation based on semi-transparent spheres for the optical properties was (optionally) implemented (namelist parameter `lrad_use_largesizeapprox`).

Several new options for calculation of water contents, effective radii and aspect ratios (both are functions of number concentration and mass concentration) for various hydrometeors were implemented. That includes:

- Estimating N_{Ca} - the number concentration of 3-dimensional hydrophilic aerosol fields using Tegen [18] or CAMS-ECMWF [1, 11] input data.
- Estimating w_{eff} - the subgrid local updraft velocity, using turbulent kinetic energy, radiative cooling and optionally convective velocity scale after Deardorff [2] (namelist parameter `lincl_wstar_in_weff`).
- Utilization of N_{Ca} and w_{eff} to calculate N_{CCN} , the number concentration of nucleated cloud droplets for computing R_e of cloud water, using the Segal-Khain method [16] (namelist parameters `icloud_num_type_rad` and `icloud_num_type_gscp`). `icloud_num_type_rad` affects the radiation indirect aerosols effect on clouds and `icloud_num_type_gscp` affects the auto-conversion rate in the 1-moment microphysical scheme.
- Number concentrations of other species (rain, cloud ice, snow and graupel) are either estimated consistently to assumptions on particle size distributions in the 1-moment cloud microphysics scheme, or are prognostic for grid scale clouds in case of the 2-moment scheme.

- "Stratiform" subgrid-scale cloud droplets and ice water contents (LWC_{sgs} and IWC_{sgs} , respectively) are estimated as functions of temperature and humidity. The shallow convection LWC_{sgs} is estimated by one of the 3 following methods: as function of temperature and humidity, similarly to stratiform clouds; as equal to the LWC of COSMO shallow convection scheme (namelist parameter `luse_qc_con_sgs`); and as fraction of the theoretical adiabatic water content [9] (namelist parameter `luse_qc_adiab_for_reffc_sgs`). The overall LWC_{sgs} is estimated by the default COSMO method as weighted average of the "stratiform" and "convective" parts, using the corresponding cloud fractions. The grid scale water contents of cloud water and ice, snow, graupel and rain are prognostic variables.
- Effective radii and aspect ratios for cloud droplets and cloud ice, as well as snow, graupel and rain are estimated as function of the corresponding water contents and number concentrations. For situations dominated by subgrid-scale shallow convection, the effective radius of subgrid-scale cloud droplets can be, alternatively, estimated using the "adiabatic" parametrization [9] (namelist parameter `luse_qc_adiab_for_reffc_sgs`).

The list of parameters of the new cloud-radiation coupling scheme is presented in Table 1 in the Appendix. The Table includes the meaning of each parameter, its type, default value, available range and recommended value.

3 Case Study

Preliminary tests of the new cloud-radiation coupling scheme (implemented in COSMO 5.5) were performed over the eastern Mediterranean (COSMO-IL domain 26-36N, 25-39E) with grid spacing of 2.8 km. The weather event was chosen to be on 16/02/2018. During that day the eastern Mediterranean was in the warm sector of a deep upper air trough approaching from the west (see satellite image in Figure 1). The SW winds caused desert dust advection into the region. The COSMO runs (driven by IFS data) were initialized on 16/2/2018 00 UTC and produced forecasts up to 16/2/2018 12 UTC.

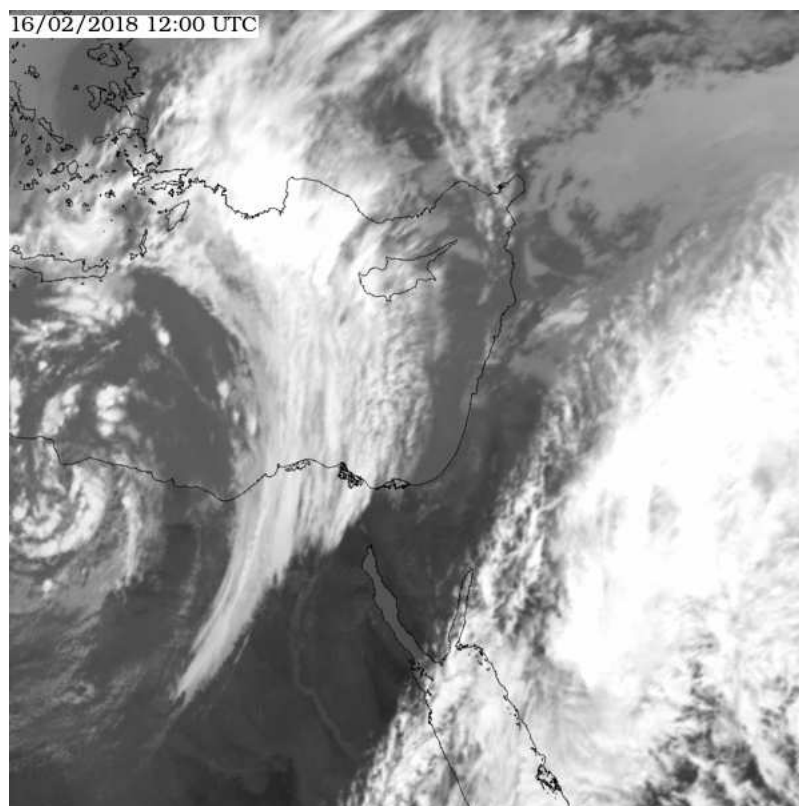


Figure 1: IR 10.8 MeteoSat satellite image for 16/2/2018 at 12 UTC.

Eight COSMO runs have been performed, with namelist parameter variations as summarized in Figure 2. The reference experiment (Ref) includes the default cloud-radiation scheme (`iradpar_cloud=1`) and Tanre aerosol climatology (`itype_aerosol=1`). Exp.1 is similar to Ref, with Tegen aerosol climatology (`itype_aerosol=2`). Exp.2 is similar to Exp. 1 with Segal-Khain estimation of cloud-droplet number concentration (`icloud_num_type_rad=2` and `icloud_num_type_gscp=2`). Exp. 3 is similar to Exp.2 with consideration of Deardorff convective velocity scale in calculation of the local subgrid-scale updraft (`lincl_wstar_in_weff=TRUE`), and with tuned hydrometeor number concentrations (`lreduce_qnx_vs_qx=TRUE`). Exp.4 is similar to Exp.3 with subgrid scale droplets and ice effective radius calculation using water contents and number concentrations (`luse_reff_ini_x_as_reffx_sgs=FALSE`), and with tuned water content reduction (`luse_tqcqitqs=TRUE`). Exp.5 is similar to Exp.4 with an estimation of shallow Cu droplets effective radius using the "adiabatic" parametrization (`luse_qc_adiab_for_reffc_sgs=TRUE`), and their water content using the shallow convection parametrization (`luse_qc_con_sgs=TRUE`). Exp.6 is similar to Exp.5 with revised asymmetry function of ice particles (`lrاد_ice_smooth_surfaces=FALSE` and `lrاد_ice_fd_is_gsquared=TRUE`). Exp.7 is similar to Exp. 6 with MCSI parameterization of spectral bands sampling in the radiation solver (`itype_mcsi=1`) compensated by more frequent calls to the radiation scheme (every 3 minutes instead of 15).

Parameter	Meaning	Ref	1	2	3	4	5	6	7
<code>iradpar_cloud</code>	type of optical prop.	1	1	4	4	4	4	4	4
<code>lrاد_incl_qrqsqg</code> <code>lrاد_use_largesizeapprox</code>	include rain, snow and graupel	F F	F F	T T	T T	T T	T T	T T	T T
<code>itype_aerosol</code>	aerosols data source	1	2	2	4	4	4	4	4
<code>icloud_num_type_rad</code> <code>icloud_num_type_gscp</code>	Segal-Khain parameterization	1 1	1 1	2 2	2 2	2 2	2 2	2 2	2 2
<code>lincl_wstar_in_weff</code>	local updraft calc.	F	F	F	T	T	T	T	T
<code>lreduce_qnx_vs_qx</code>	tune number conc.	F	F	F	T	T	T	T	T
<code>luse_reff_ini_x_as_reffx_sgs</code>	effective radius calc.	T	T	T	T	F	F	F	F
<code>luse_tqcqitqs</code>	tune water content	F	F	F	F	T	T	T	T
<code>luse_qc_adiab_for_reffc_sgs</code>	new paramet. for Cu	F	F	F	F	F	T	T	T
<code>luse_qc_con_sgs</code>	shall. C. LWC for Cu	F	F	F	F	F	T	T	T
<code>lrاد_ice_smooth_surfaces</code> <code>lrاد_ice_fd_is_gsquared</code>	ice particles roughness	T F	T F	T F	T F	T F	T F	F T	F T
<code>itype_mcsi</code>	MCSI paramet.	0	0	0	0	0	0	0	1

Figure 2: Summary of the eight COSMO experiments.

The sensitivity results of the COSMO runs are presented in 3 as function of the forecast range. The upper left panel presents the averaged global radiation over the cloudy grid points (cloud cover > 0.1). For each experiment the global radiation of the Ref run is subtracted, showing the sensitivity effect of the current experiment. The upper right panel presents similar results for the averaged 2 meter temperature. Similarly, the lower panels present the sensitivity results for the clear sky regions (cloud cover < 0.1), highlighting the direct effects of aerosols and the MCSI parameterization.

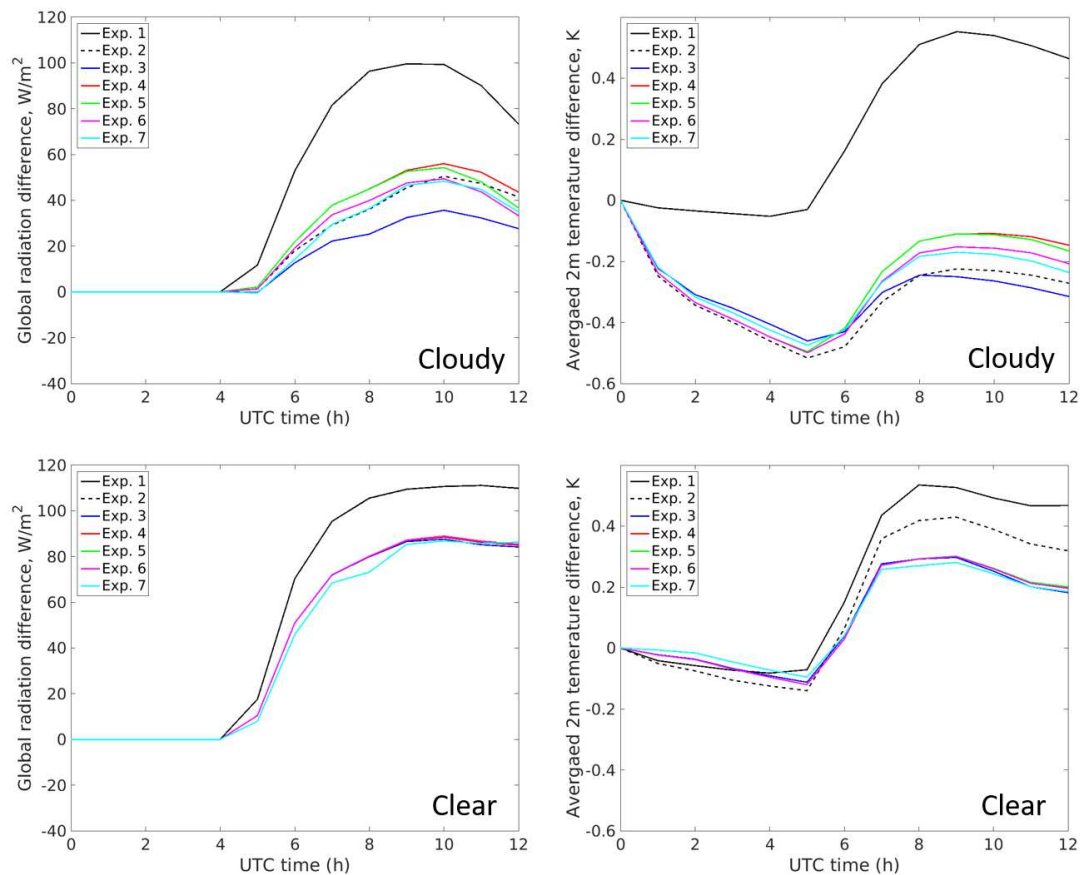


Figure 3: Sensitivity results of the COSMO runs as function of the forecast range. The upper left panel presents the averaged over the cloudy grid points (cloud cover > 0.1) global radiation. For each experiment the global radiation of the Ref run is subtracted, showing the sensitivity effect of the current experiment. The upper right panel presents similar results for the averaged 2 meter temperature. Similarly, the lower panels present the sensitivity results for the clear sky regions (cloud cover < 0.1).

One can see (Exp. 1) that the use of Tegen aerosol instead of Tanre strongly increases the global radiation (up to 120 W/m^2) and the 2 meter temperature up to 0.5 K. Exp. 2 shows that in the cloudy areas the new optical properties and Segal-Khain nucleation, and – most importantly – consideration of rain, snow and graupel particles in radiation, decreases the enhancement to about 50 W/m^2 . Exp. 3 shows that in the cloudy areas revision of the local updraft for Segal-Khain nucleation and tuning the number concentration SGS decreases the enhancement further to about 35 W/m^2 . Exp. 4 shows that in the cloudy areas revision of SGS effective radius calculations and imposing upper limits to the total water contents brings the enhancement back to about 50 W/m^2 . Experiments 5,6 and 7 show smaller sensitivity on average. Generally, one can see that the new cloud-radiation coupling scheme affects the global radiation by $30\text{-}120 \text{ W/m}^2$ which corresponds to a 2 meter temperature variation range of about 1 K. Important to note is, that these results are preliminary and reflect the model sensitivity at a single day over a specified region only. Also, the results include averaging over large areas, which suggests much higher sensitivities locally. We should also note that this is the first attempt to test the code within the 5.5 framework. Each of the new scheme components was massively tested within the 5.1 framework. In the appendix we provide the "recommended" namelist based on the studies during the last 4-years, which were discussed and published in various presentations and papers, as can be viewed on $T^2(RC)^2$ web page (<http://www.cosmo-model.org/content/tasks/priorityProjects/t2rc2/default.htm>).

4 Summary

In this short article we inform the COSMO community about the recent implementation of a revised cloud-radiation coupling scheme into COSMO 5.5. Officially this code will be distributed with the final version of COSMO - COSMO-6. The new scheme includes an optional modification to the radiation solver (MCSI

parametrization). It further includes implementation of new aerosol climatologies and prognostic aerosol fields which modify the clear sky optical properties. Moreover, the indirect effect of aerosols on number concentrations, effective radii and water contents in grid and subgrid scale clouds is significantly revised. The optical properties of solid and water hydrometeors for the different spectral intervals were revised as well. Preliminary tests show a significant effect of the new cloud-radiation coupling scheme on radiation and 2 meter temperature.

Acknowledgments

Besides the authors, the new cloud-radiation coupling code includes important contributions from Simon Gruber (KIT), Alexey Poliukov (MSU), Natalia Chubarova (MSU), Marina Shatunova (Roshydromet), Ulrich Schaettler (DWD), Daniel Rieger (DWD), Martin Kohler (DWD), Alon Shtivelman (IMS), Yoav Levi (IMS), Xavier Lapillonne (MeteoSwiss), Oliver Fuhrer (MeteoSwiss), Gdaly Rivin (Roshydromet), Alexander Kirsanov (Roshydromet), Matthias Raschendorfer (DWD), Ralph Becker (DWD), Stefan Kinne (MPI-Met Hamburg), Daniel Luthi (DWD), Alessio Bozzo (ECMWF), Alexander Khain (HUJI), Bodo Ritter (DWD), Dmitrii Mironov (DWD) and Bernard Vogel (KIT). The COSMO priority project $T^2(RC)^2$ was led by Harel Muskatel (IMS).

References

- [1] Benedetti, A., J.-J. Morcrette, O. Boucher, A. Dethof, R. J. Engelen, M. Fisher, H. Flentje, N. Huneeus, L. Jones, J. W. Kaiser, et al., 2009: Aerosol analysis and forecast in the European Centre for Medium-Range Weather Forecasts Integrated Forecast System. Part 2: Data assimilation, *J. Geophys. Res.-Atmospheres*, 114(D13), D13205, doi:10.1029/2008JD011115.
- [2] Deardorff, J. W.: 1970, 'Convective Velocity and Temperature Scales for the Unstable Planetary Boundary Layer and for Rayleigh Convection', *J. Atmos. Sci.* 27, 1211–1213.
- [3] Doms, G., J. Forstner, E. Heise, H.-J. Herzog, D. Mironov, M. Raschendorfer, T. Reinhardt, B. Ritter, R. Schrodin, J.-P. Schulz and G. Vogel, 2011: A description of the Nonhydrostatic Regional COSMO Model. Part II: Physical Parameterization. Deutscher Wetterdienst, 161 pp.
- [4] Fu, Q., and Liou, K. N. (1992), A threeparameter approximation for radiative transfer in nonhomogeneous atmospheres: Application to the O₃ 9.6m band, *J. Geophys. Res.*, 97(D12), 13051– 13058, doi:10.1029/92JD00999.
- [5] Fu Q., 1996, An Accurate Parameterization of the Solar Radiative Properties of Cirrus Clouds for Climate Models, *J. Clim.*, 9, 2058-2082
- [6] Fu Q., P. Yang and W. B. Sun, 1998, An Accurate Parameterization of the Infrared Radiative Properties of Cirrus Clouds for Climate Models, *J. Clim.*, 11, 2223-2237
- [7] Fu Q., 2007, A New Parameterization of an Asymmetry Factor of Cirrus Clouds for Climate Models, *J. Atm. Sci.*, 64, 4140-4150
- [8] Hu, Y.X. and K. Stamnes, 1993: An Accurate Parameterization of the Radiative Properties of Water Clouds Suitable for Use in Climate Models. *J. Climate*, 6, 728–742, [https://doi.org/10.1175/1520-0442\(1993\)006<0728:AAPOTR>2.0.CO;2](https://doi.org/10.1175/1520-0442(1993)006<0728:AAPOTR>2.0.CO;2)
- [9] Khain, P., R. Heiblum, U. Blahak, Y. Levi, H. Muskatel, E. Vadislavsky, O. Altaratz, I. Koren, G. Dagan, J. Shpund, and A. Khain, 2019: Parameterization of Vertical Profiles of Governing Microphysical Parameters of Shallow Cumulus Cloud Ensembles Using LES with Bin Microphysics. *J. Atmos. Sci.*, 76, 533–560, <https://doi.org/10.1175/JAS-D-18-0046.1>
- [10] Kinne, S., D. O'Donnell, P. Stier, S. Kloster, K. Zhang, H. Schmidt, S. Rast, M. Giorgetta, T. F. Eck, and B. Stevens (2013), MAC-v1: A new global aerosol climatology for climate studies, *J. Adv. Model. Earth Syst.*, 5, 704740, doi:10.1002/jame.20035.
- [11] Morcrette, J.-J., O. Boucher, L. Jones, D. Salmond, P. Bechtold, A. Beljaars, A. Benedetti, A. Boner, J. W. Kaiser, M. Razinger, et al., 2009: Aerosol analysis and forecast in the European Centre for Medium-Range Weather Forecasts Integrated Forecast System. Part 1: Forward modelling, *J. Geophys. Res.-Atmospheres*, 114(D6), D06206, doi:10.1029/2008JD011235.

- [12] Mueller R., C. Träger-Chatterjee, Brief Accuracy Assessment of Aerosol Climatologies for the Retrieval of Solar Surface Radiation, *Atmosphere* 2014, 5, 959-972; doi:10.3390/atmos5040959
- [13] Pincus, R., and Stevens, B. (2009), Monte Carlo Spectral Integration: a Consistent Approximation for Radiative Transfer in Large Eddy Simulations, *J. Adv. Model. Earth Syst.*, 1, 1, doi:10.3894/JAMES.2009.1.1.
- [14] Rieger, D., Bangert, M., Bischoff-Gauss, I., Förstner, J., Lundgren, K., Reinert, D., Schröter, J., Vogel, H., Zängl, G., Ruhnke, R., and Vogel, B.: ICON-ART 1.0 – a new online-coupled model system from the global to regional scale, *Geosci. Model Dev.*, 8, 1659-1676, <https://doi.org/10.5194/gmd-8-1659-2015>, 2015.
- [15] Ritter, B. and J. Geleyn, 1992: A Comprehensive Radiation Scheme for Numerical Weather Prediction Models with Potential Applications in Climate Simulations. *Mon. Wea. Rev.*, 120, 303–325, [https://doi.org/10.1175/1520-0493\(1992\)120<0303:ACRSFN>2.0.CO;2](https://doi.org/10.1175/1520-0493(1992)120<0303:ACRSFN>2.0.CO;2)
- [16] Segal, Y., and Khain, A. (2006), Dependence of droplet concentration on aerosol conditions in different cloud types: Application to droplet concentration parameterization of aerosol conditions, *J. Geophys. Res.*, 111, D15204, doi:10.1029/2005JD006561.
- [17] Tanre, D., J.-F. Geleyn, and J. Slingo, 1984. First results of the introduction of an advanced aerosol-radiation interaction in the ECMWF low resolution global model. In *Proc. of the Meetings of Experts on Aerosols and their Climatic Effects*, Williamsburg, VA, pp. 133177. WMO and IAMAP.
- [18] Tegen, I., P. Hoorig, M. Chin, I. Fung, D. Jacob, and J. Penner (1997), Contribution of different aerosol species to the global aerosol extinction optical thickness: Estimates from model results, *J. Geophys. Res.*, 102, 23,895–23,915.

Appendix

The list of parameters of the new cloud-radiation coupling scheme is presented in Table 1. The Table includes the meaning of each parameter, its type, default value, available range and recommended value.

Parameter	Meaning	Type	Def	Range	Recom
iradpar_cloud	Calculation of optical properties for solid and water particles. 1-old, 4-new. 2,3 are possible but not recommended	INT	1	1,4	4
lrاد_ice_smooth_surfaces	Effective if iradpar_cloud=4. If T assume smooth surfaces for solid species (fd>0), otherwise assume rough surfaces (fd close to 0)	LOG	T	T/F	F
rad_ice_fd_is_gsquared	Effective if iradpar_cloud=4 and lrاد_ice_smooth_surfaces=T. If T compute forward scattered fraction as $f = g^2$ (RG92 method), otherwise compute $f = 1/(2\omega) + f_d$ with $f_d = fct(AR)$ according to the new fits. Concerns only the solar frequency bands	LOG	F	T/F	F
lrاد_incl_qrqsqg	include/exclude QR, QS and QG in radiative transfer calculations	LOG	F	T/F	T
lrاد_use_largesizeapprox	Effective for iradpar_cloud = 4: if F new fits for all optical properties of solid species are used without clipping. If T only for the extinction the large-size approximation is applied starting from Reff=150 microns	LOG	T	T/F	T
itype_aerosol	Type of aerosol map. Climatology: 1-Tanre, 2-Tegen, 3-Kinne. Prognostic data from int2lm: 4-CAMS, 5-ART	INT	1	1-5	4

icloud_num_type_rad	Derivation of cloud number concentration for radiation. 1: use cloud_num_rad tuning parameter. 2: derive from Tegen/CAMS aerosol data using Segal-Khain parametrization (effective for itype_aerosol=2,4 only)	INT	1	1,2	2
icloud_num_type_gscp	Derivation of cloud number concentration for 1-moment microphysics. 1: use cloud_num tuning parameter. 2: derive from Tegen/CAMS aerosol data using Segal-Khain parametrization (effective for itype_aerosol=2,4 only)	INT	1	1,2	2
lincl_wstar_in_weff	Effective in case of icloud_num_type_rad/gscp=2 (Segal-Khain). If T, the eff. w for cloud nucleation is enforced to be $\geq w^*$ (conv. vel. scale in PBL), but only below the PBL height or below the upper bound of the lowest "convective cloud layer", whichever is higher. F - otherwise	LOG	F	T/F	T
cloud_num_rad	Tuning parameter for cloud number concentration for radiation ($1/m^3$)	REAL	2E8	[0.1-10]E8	2E8
cloud_num	Tuning parameter for cloud number concentration for 1-moment microphysics ($1/m^3$)	REAL	5E8	[0.1-10]E8	5E8
zref_cloud_num_rad	Height of lower layer (above MSL in m) above which the cloud number concentration is exponentially reduced with height	REAL	2000	500-3000	2000
dz_oe_cloud_num_rad	1/e decrease height in m of exponential decrease of cloud number concentration above zref_cloud_num_rad	REAL	2000	500-3000	2000
lreduce_qnx_vs_qx	T: reduce qnx vs qx for radiation. In this case the 9 tuning parameters below are activated. F: otherwise	LOG	F	T/F	T
rhoc_nhigh_rad	For $q_c \leq \text{rhoc_nhigh_rad}$, q_{nc} is not reduced as function of q_c [kg/m^3]	REAL	0.5 E-4	[0.1-20] E-4	0.5 E-4
rhoc_nlow_rad	For $\text{rhoc_nhigh_rad} < q_c < \text{rhoc_nlow_rad}$ q_{nc} is linearly reduced as function of q_c [kg/m^3]	REAL	2.0 E-4	[0.1-20] E-4	2.0 E-4
nfact_low_rad	For $q_c \geq \text{rhoc_nlow_rad}$, the linear reduction bottoms out at the nfact_low_rad'th fraction of q_{nc}	REAL	0.1	[0...1]	0.1
rhoi_nihigh_rad	For $q_i \leq \text{rhoi_nihigh_rad}$, $n_i(T)$ is not reduced as function of q_i [kg/m^3]	REAL	0.5 E-5	[0.1-20] E-5	0.5 E-5
rhoi_nilow_rad	For $\text{rhoi_nihigh_rad} < q_i < \text{rhoi_nilow_rad}$, $n_i(T)$ is linearly reduced as function of q_i [kg/m^3]	REAL	2.0 E-5	[0.1-20] E-5	2.0 E-5
nifact_low_rad	For $q_i \geq \text{rhoi_nilow_rad}$, the linear reduction bottoms out at the nifact_low_rad'th fraction of $n_i(T)$	REAL	0.1	[0...1]	0.1
rhos_n0shigh_rad	For $q_s \leq \text{rhos_n0shigh_rad}$, n_{0s} is not reduced as function of q_s [kg/m^3]	REAL	1.0 E-5	[0.1-20] E-5	1.0 E-5
rhos_n0slow_rad	For $\text{rhos_n0shigh_rad} < q_s < \text{rhos_n0slow_rad}$, n_{0s} is linearly reduced towards $n_{0s_low_rad}$ [kg/m^3]	REAL	5.0 E-5	[0.1-20] E-5	5.0 E-5
n0s_low_rad	For $q_s \geq \text{rhos_n0slow_rad}$, n_{0s} attains this const. value [m^{-3}]	REAL	8 E5	[1-50] E5	8 E5
luse_reff_ini_x_as_reffx_sgs	Use tuning parameters reff_ini_c, reff_ini_i for SGS eff. radius	LOG	T	T/F	F

reff_ini_c	Effective radius for SGS cloud droplets (m). Only if luse_reff_ini_x_as_reffx_sgs=T	REAL	5 E-6	[3-15] E-6	5 E-6
reff_ini_i	Effective radius for SGS cloud ice (m). Only if luse_reff_ini_x_as_reffx_sgs=T	REAL	10 E-6	[5-30] E-6	10 E-6
radqc_fact, radqi_fact, radqs_fact, radqg_fact	Portion of GS and SGS qc, qi, qs, qg (respectively) "seen" by the radiation. Should be <1 because of subgrid-scale variability. Increase leads to higher optical thickness	REAL	0.5	[0.5-1]	0.5
qvsatfact_sgscl_rad	Scaling factor for qc and qi of SGS clouds: local supersaturation which is assumed to have been depleted by SGS cloud formation [-]. Increase leads to higher optical thickness	REAL	0.01	[0.005-0.02]	0.01
luse_tqctqitqs	limit TQC, TQI, TQS to some integral maximum. Adjust qc, qi, qs accordingly (for radiation). T leads to lower optical thickness	LOG	F	T/F	T
luse_qc_adiab_for_reffc_sgs	Use "adiabatic" parametrization for SGS shallow convection effective radius	LOG	F	T/F	T
luse_qc_con_sgs	Effective if luse_qc_adiab_for_reffc_sgs=T. LOG F: use "adiabatic" parametrization for SGS shallow convection LWC. T: use LWC from shallow convection parametrization (if lconv=T)	LOG	F	T/F	T
alpha1_adiab_rad	Linear deviation with height (above cloud base) of SGS shallow convection effective radius from the adiabatic value alpha1_adiab_rad-alpha2_adiab_rad*(z-zcb). [-]	REAL	0.95	[0.7-1]	0.95
alpha2_adiab_rad	Linear deviation with height (above cloud base) of SGS shallow convection effective radius from the adiabatic value alpha1_adiab_rad-alpha2_adiab_rad*(z-zcb). [1/m]	REAL	1.2 E-4	[1-2] E-4	1.2 E-4
beta_adiab_rad	Ratio of cloud-average number concentration (of SGS shallow convection) with respect to the cloud core value (obtained from Segal-Khain)	REAL	0.38	[0.2-1]	0.38
gamma_adiab_rad	Linear deviation with height (above reff=12micron level) of SGS shallow conv. qc from the "pseudo-adiabatic" value. [1/km]	REAL	0.45	[0.2-0.7]	0.45
itype_mcsi	1: Monte Carlo Spectral Integration in the radiation solver. Recommended together with ninrad=5. 0-Default from RG92	INT	0	0,1	0

Table 1: List of parameters of the new cloud-radiation coupling scheme. The parameters are separated to groups according the corresponding parametrization: Optical properties derivation; Effect of large hydrometeors on radiation; Aerosols effect in clear sky and on droplets number concentration in clouds; Reduction of hydrometeors number concentrations for large water contents; Method of effective radius calculation; Tuning water contents "seen" by radiation; "Adiabatic" parametrization for liquid water content and effective radius in shallow cumulus; New method for radiation solver. The Table includes the meaning of each parameter, its type, default value, available range and recommended value.